CASE STUDY OF SPUDCAN RE-PENETRATION ANALYSIS USING LARGE DEFORMATION FINITE ELEMENT APPROACH

K.K. Tho*, N. Chan
FUGRO SINGAPORE

Y. Zhou, J. Liu and S. Zhou
CHINA OILFIELD SERVICES LIMITED

** corresponding author: k.tho@fugro.com*

ABSTRACT
A jack-up re-entry into existing footprints warrants a new set of spudcan penetration curves to be generated. In a uniform clay profile, the spudcan re-penetration analysis will typically be performed by applying a degradation factor to the intact strength profile adopted for the original spudcan penetration analysis. However, in layered soil profiles such as those consisting of sand overlying clay, bearing capacity calculation of spudcan re-entry into an existing footprint is complicated by changes in the soil layering during the first penetration. This paper presents a case study of a spudcan re-penetration analysis in a sand overlying clay soil profile using large deformation finite element approach. Spudcan penetration, extraction and re-penetration activities are sequentially simulated in a single numerical model. The degradation of soil strength in clay is modelled using a strain-softening constitutive model. Changes in soil layering and the development of cavity within the footprint are implicitly accounted for in the numerical simulation. The numerically predicted spudcan penetration depth is found to agree well with the actual spudcan penetration depth. This case study demonstrates that large deformation finite element is a viable tool for preforming spudcan re-penetration analysis in layered soil profiles.

KEY WORDS: jack-up, re-entry, penetration, large deformation, finite element, sand overlying clay

INTRODUCTION

Due to operational and scheduling requirements, it was necessary for a jack-up rig to reenter a location at South China Sea within six months. This site was previously visited by the same jack-up rig and the plan, guided by recommendations of SNAME (2008), was to re-enter at exactly the footprints of the previous visits. A jack-up re-entry into existing footprints warrants a new set of spudcan penetration curves to be generated. In a uniform clay profile, the spudcan re-penetration analysis will typically be performed by applying a degradation factor to the intact strength profile adopted for the original spudcan penetration analysis. However, in layered soil profiles such as those consisting of sand overlying clay, bearing capacity calculation of spudcan re-entry into an existing footprint is complicated by changes in the soil layering during the first penetration. Sand overlying clay soil profile is typically associated with punch-through risk during preloading and the computation of load-penetration response is usually performed in accordance with methods detailed in SNAME (2008) and ISO-19905-1 (2012). These methods are based on "wished-in-place" simplification that neglects the changes in soil stratigraphy during spudcan penetration. On the contrary, it has been demonstrated in both physical modelling experiments (Teh et al., 2008; Lee, 2009) and large deformation finite element analysis (LDFE) (Tho, 2012) that a sand plug is extruded as the spudcan penetrates through the upper sand layer. The presence of this sand plug beneath an advancing spudcan significantly alters the penetration and re-penetration response. This paper presents a case study of a spudcan re-penetration analysis in a sand overlying clay soil profile using LDFE approach.

SITE CONDITION

The soil investigation, performed prior to the first jack-up rig emplacement, consists of one 140-m sample borehole and one 140-m continuous in-situ PCPT borehole. A summary of the major soil strata up to a depth of 47.7m, as extracted from the geotechnical log, is reproduced in Table 1.

Table 1: Soil Stratigraphy

Stratum	Penetration (m)		Thickness (m)	Description
	From	To		
1	0.0	2.4	2.4	Loose fine SAND
2	2.4	5.3	2.9	Medium dense silty fine SAND
3	5.3	11.1	5.8	Laminated/Interlayered firm silty CLAY and sandy SILT
4	11.1	18.2	7.1	Firm silty CLAY
5	18.2	24.0	5.8	Medium dense sandy SILT
6	24.0	31.2	7.2	Stiff silty CLAY
7	31.2	35.1	3.9	Medium dense silty fine SAND
8	35.1	40.9	5.8	Interlayered/laminated medium dense sandy SILT/silty fine SAND and stiff silty CLAY
9	40.9	43.0	2.1	Stiff silty CLAY
10	43.0	47.7	4.7	Medium dense silty fine SAND

The soil conditions at the site consist of alternating layers of sands/sandy silts and clays from mudline to 108.7m; sand and silt layers are present from 108.7m to final investigated depth of 140.0m. The sands/sandy silts are generally medium dense to dense in relative density. The shallow soil stratigraphy consists of a loose sand layer from mudline to 2.4m and a medium dense sand layer from 2.4 to 5.3m. These sand layers overlay laminated firm clays and silts from 5.3 to 11.1m and firm clay layer from 11.1 to 18.2m.

SPUDCAN DETAILS

The rig used at this site is a Friede and Goldman JU-2000E three-legged jack-up drilling rig. Each independent leg consists of a structural truss fitted with a spud-type tank footing of approximately circular shape at the lower end. The equivalent diameter of the spudcan is 18m and the maximum spudcan reaction per leg is 110MN.

LARGE DEFORMATION FINITE ELEMENT ANALYSIS

Numerical analysis of continuous deep spudcan penetration is a fundamentally challenging problem involving severe mesh distortion in finite element analysis due to very large soil deformation, complex contact conditions and nonlinear soil behaviour. Conventional Lagrangian-based large strain, large deformation finite element analysis is not viable due to severe mesh distortion arising from very large soil deformations. The ABAQUS Coupled Eulerian-Lagrangian (CEL) finite element approach is adopted in this study.

In an Eulerian analysis, the spatial position of the nodes is fixed and the finite element mesh undergoes zero distortion during the analysis. Instead, materials are allowed to move (flow) from one element to another element during the analysis. Owing to the large deformation characteristic of the spudcan penetration problem,

the Eulerian approach is an attractive solution strategy. The problem associated with severe mesh distortion in the case of a Lagrangian analysis is circumvented in an Eulerian analysis.

The Eulerian time incrementation algorithm is based on an operator split of the governing equations, resulting in a traditional Lagrangian phase followed by an Eulerian phase. As with the case of Arbitrary Lagrangian Eulerian (ALE) technique, a standard large deformation explicit Lagrangian finite element analysis is conducted in the first step. In the second step which is an Eulerian step, advection is performed where the solution variables (such as stress, strain, etc) are mapped from the deformed mesh back to the original mesh. Further details on the applicable of CEL technique to simulate spudcan penetration can be found in Qiu et al. (2011) and Tho et al. (2012).

A three-dimensional finite element model is created in ABAQUS Version 6.13-3. Pre and post-processing are carried out in ABAQUS/CAE. After the input file is generated, the ABAQUS/Explicit solver with coupled Eulerian-Lagrangian capability is employed for the analysis. In order to minimize the computational cost, only one-eighth of the domain is modelled as shown in Figure 1. In the Eulerian soil domain, it is necessary to define a layer known as void above the mudline. The void layer consists of Eulerian brick elements that are initially empty. The purpose of the void layer is to allow the soil to heave and flow into the initially empty Eulerian elements at subsequent stages of the analysis.

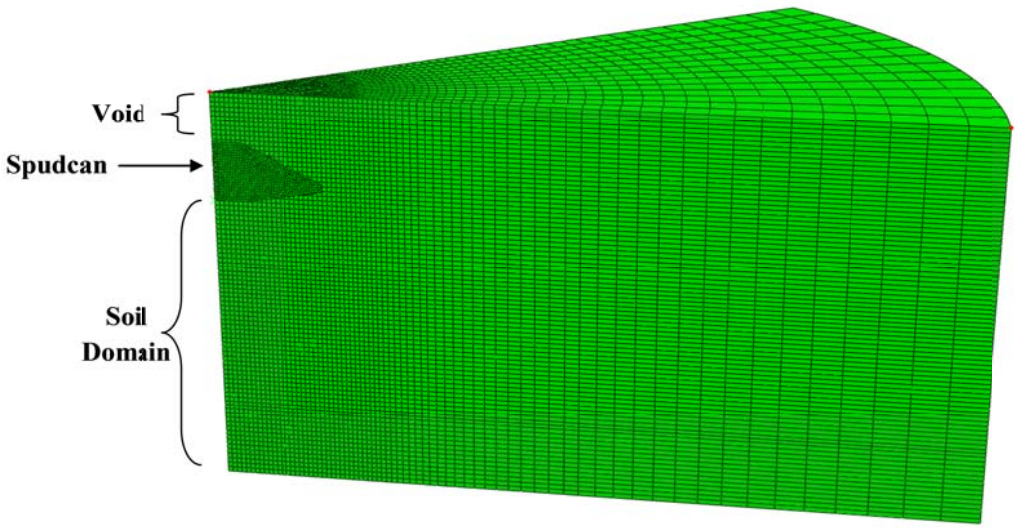

Figure 1: Eulerian Finite Element Model

Symmetric radial boundary conditions in the form of zero velocity normal to the plane of symmetry are imposed on the two planes of symmetry. Tangential velocity is constrained to be zero at the curved face at the far-field boundary. The soil domain is modelled as an Eulerian part while the spudcan is modelled as a Lagrangian part. The soil-spudcan contact interaction is imposed through the Coupled Eulerian Lagrangian functionality in ABAQUS.

By taking into consideration of the maximum observed penetration depth of 15.5m coupled with the presence of medium dense sand layers from the depth of 18.2 m to 24.0m, the bottom boundary of the soil domain is set to be equal to the base of the sand layer at a depth of 24.0m from the mudline. By optimising on the depth of soil domain in the finite element model, a finer mesh can be used within the domain of interest to generate more accurate results. The radial boundary is fixed at 63m from the centreline of the spudcan to avoid errors arising from boundary effect.

For enhanced computational efficiency, the spudcan is modelled as a rigid solid part instead of using solid deformable brick elements which is computationally more time consuming. An actual spudcan consists of steel plates reinforced with internal stiffeners and is designed to withstand the maximum design preload pressure while undergoing negligible deformation. Therefore, the idealization of the spudcan as a perfectly rigid part in the numerical model should not adversely affect the accuracy of the results in terms of the displacement field generated and the corresponding pile response. On the other hand, such idealization would not be appropriate if the local stresses of the spudcan structure are of primary interest. The installation of the spudcan was modelled as a continuous spudcan penetration problem ("pushed-in-place") with the spudcan initially positioned at the mudline and progressively pushed downward to the final penetration. The extraction process is modelled with the same methodology.

The design soil parameters used in the FE analysis are presented in Table 2. For sand layers, the friction angle (ϕ') is estimated based on the cone resistance, q_c and vertical effective stress. The elastic modulus (E') is correlated to the cone resistance, q_c. For very soft clays, the E_u/c_u ratio is taken as 150, whilst for firm clay, E_u/c_u ratio of 200 is deemed applicable where E_u is the undrained elastic modulus.

Table 2: Summary of Soil Parameters for LDFE Analysis

Layer No.	Ground Behaviour	Depth (m)		γ (kN/m^3)	ϕ' (deg)	c_u (kPa)		E (kPa)
		Top	Bot			Top	Bot	
1	Cohesive	0.0	1.2	18.8	-	5.0	5.0	750
2	Frictional	1.2	5.3	18.5	30	-	-	20000
3	Cohesive	5.3	8.3	17.1	-	40	40	8000
4	Cohesive	8.3	11.1	17.1	-	50	50	10000
5	Cohesive	11.1	18.2	17.7	-	45	45	9000
6	Frictional	18.2	24.0	19.0	25	-	-	20000

A Poisson's ratio of 0.3 was used in the sand layers and 0.495 in the clay layers.

Sand layers have been modelled as a drained material with the Mohr-Coulomb yield criterion and non-associated flow with zero angle of dilation.

In order to simulate the phenomena of progressive strength degradation with increasing accumulation of plastic deformation, a modified Tresca material model with strain-softening is adopted to model the clay layers. The Tresca constitutive model incorporating a widely used exponential strain softening relationship [Einav and Randolph, 2005; Zhou and Randolph, 2007; Wang et al., 2009] is employed in the finite element model as follow:

$$s_u = \left[\frac{1}{S_t} + \left(1 - \frac{1}{S_t}\right) e^{\frac{-3\xi}{\xi_{95}}}\right] s_{uo} \tag{1}$$

where s_{uo} is the initial undisturbed undrained shear strength; S_t is the sensitivity; ξ denotes the accumulated plastic strain and ξ_{95} represents the value of ξ at which soil has undergone 95% of total strength reduction. Unlike conventional Tresca constitutive model where the soil strength remains constant throughout the analysis,

this improved constitutive model enables the effect of progressive strength degradation from the intact undrained shear strength towards the remoulded undrained shear strength with increasing accumulation of plastic deformation to be simulated. The parameter ξ_{95} governs the rate at which the strength degrades from intact strength to remoulded strength. Typical values of ξ_{95} are reported to be in the range of 10-30 [Wang et al., 2009]. The rate of strength degradation varies inversely with the value of ξ_{95}. In this study, a value of 10 is adopted.

The spudcans have been idealized as circular in plan and of equivalent area to the actual spudcan of the subject rig. Prescribed displacements are applied onto the spudcan model to simulate the continuous penetration and extraction and re-penetration processes. In order to simulate the disturbed condition within the soil mass in the vicinity of the footprint during the jack-up re-entry, spudcan penetration and extraction of the first jack-up rig deployment was modelled. The spudcan was penetrated to a tip penetration depth of 13.5m before performing a full extraction. The reaction force arising from the applied prescribed displacement is extracted as an output from the finite element analysis.

RESULTS AND DISCUSSIONS

The results from the LDFE analysis will first be discussed qualitatively followed by quantitative comparison of penetration depths at maximum preload. Figure 2a to 2e illustrates the change in stratigraphy and the associated soil flow mechanisms at spudcan tip penetration depths of 1.5m, 4.5m, 7.5m, 10.5m and 13.5m. The upper sand layer is shown in red while the clay layers are shown in blue. Due to the limitation of ABAQUS/CAE, it was not possible to assign a different colour to more than two material types. As a workaround, the region occupied by the lower sand layer is assigned a different shading for ease of reference. The instantaneous velocity vectors, which provide indication of operative soil flow mechanism, are overlaid on these figures.

As illustrated in Figure 2a, the thin upper soft clay layer is squeezed out as the spudcan penetrates into the soil. Figure 2b shows the spudcan penetrating through the upper sand layer. An inverted cone wedge is evident in the clay beneath the sand layer directly below the spudcan. At a spudcan penetration depth of 7.5m (shown in Figure 2c), the sand plug trapped beneath the spudcan has almost completely separated from the upper sand layer. It can also be observed that the upper sand layer is flowing to the upper surface of the spudcan. A well-developed slip plane in the clay layer is also apparent. As the spudcan penetrates to 10.5m (shown in Figure 2d), the lower part of slip plane in the clay layer is intercepted by the lower sand layer. At the final penetration depth of 13.5, it can be observed that the composite footing formed by the spudcan and the underlying sand plug is squeezing the clay layer against the lower sand layer. A constrained flow mechanism is evident in the vicinity of the composite footing.

Figure 3 shows the soil stratigraphy after full spudcan extraction. It can be observed that the thickness of the upper sand layer in the vicinity of the spudcan footprint reduces significantly and a substantial amount of heaving occurred. This is due to the collapse of sand adjacent to the spudcan into the crater during spudcan extraction. The sand within the footprint composed of those pushed down beneath the spudcan during spudcan penetration and those deposited during spudcan extraction. The sand and clay within the footprint are intermixed.

During the spudcan re-penetration, the outer edge of the spudcan comes into contact with the soil within the footprint at a depth of approximately 4.5m (Figure 4a). As the spudcan penetrates deeper, the sand beneath the spudcan is being squeezed out and flow together with the clay (Figure 4b and 4c). This behaviour is different from those observed during the first spudcan penetration whereby the sand beneath the spudcan formed a composite footing with the spudcan. This difference in flow mechanism could be attributed to the fact that the sand within the footprint deposited during spudcan extraction is intermixed with the clay and hence are weaker than the homogeneous sand plug that is pushed ahead of the spudcan during penetration. The constrained flow mechanism is again operative as the spudcan approaches the lower sand layer, as illustrated in Figures 4d and 4e.

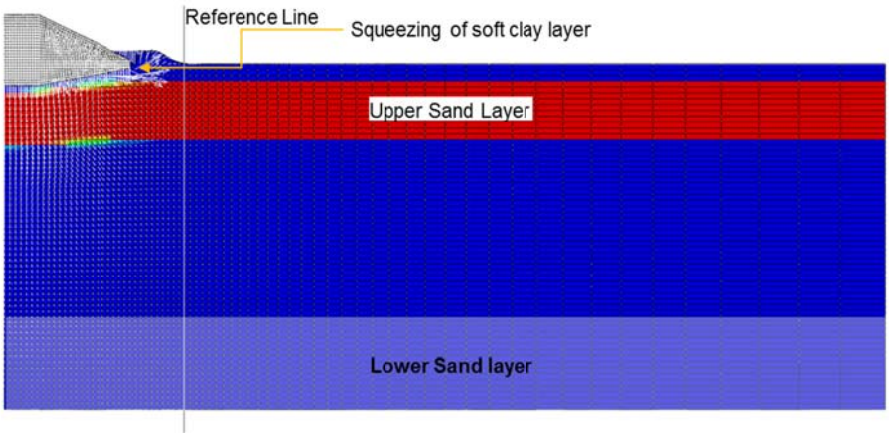

Figure 2a: Spudcan Penetration Depth = 1.5m (First Jack-up Deployment)

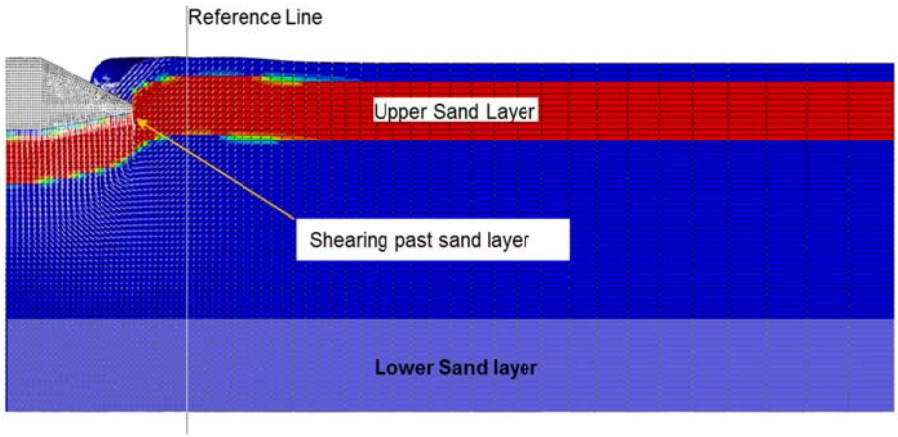

Figure 2b: Spudcan Penetration Depth = 4.5m (First Jack-up Deployment)

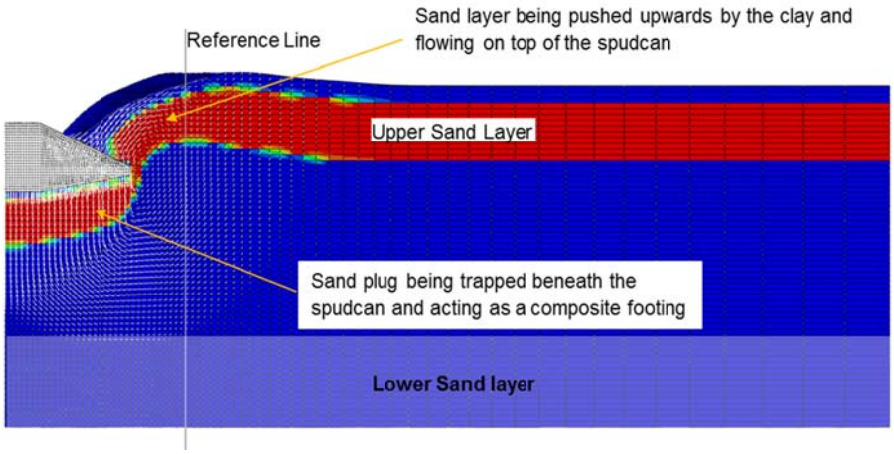

Figure 2c: Spudcan Penetration Depth = 7.5m (First Jack-up Deployment)

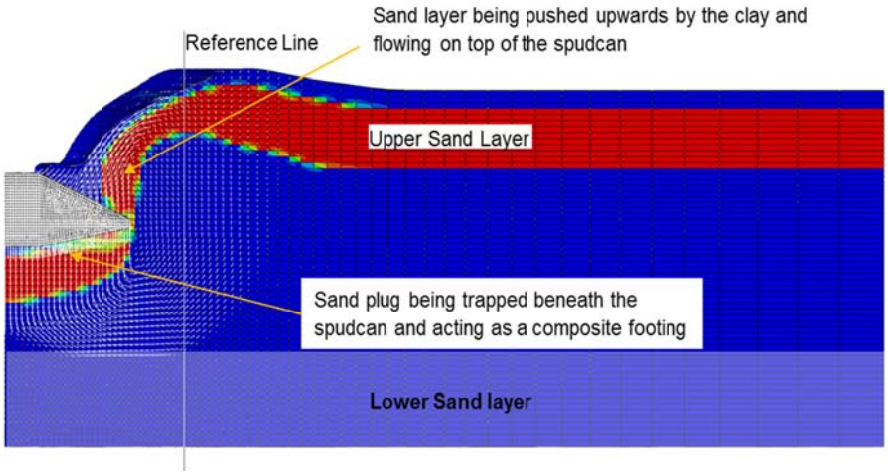

Figure 2d: Spudcan Penetration Depth = 10.5m (First Jack-up Deployment)

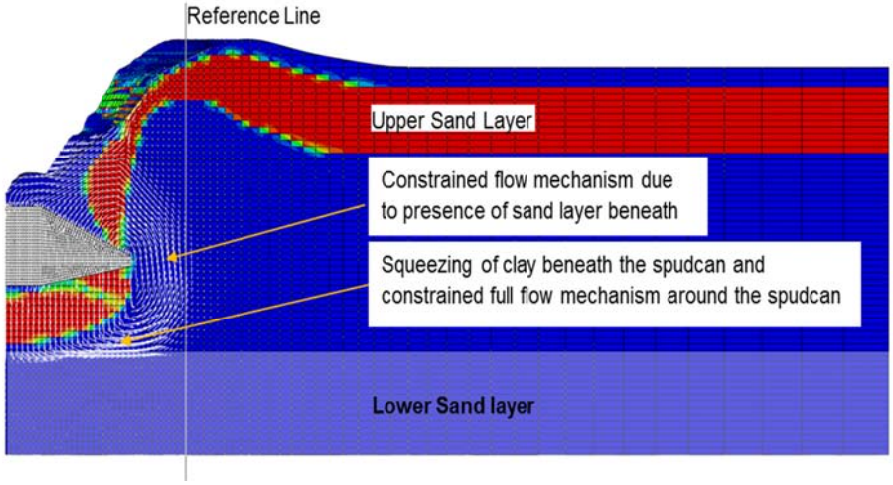

Figure 2e: Spudcan Penetration Depth = 13.5m (First Jack-up Deployment)

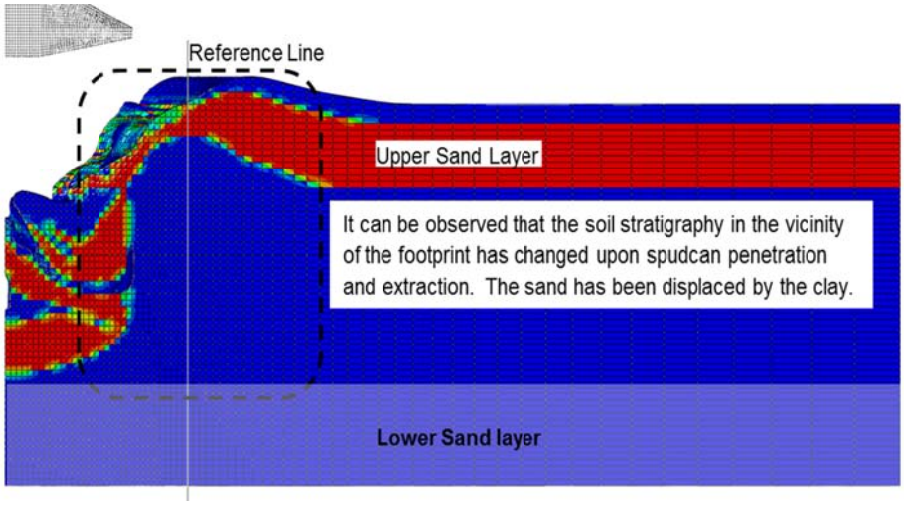

Figure 3: After Full Spudcan Extraction (First Jack-up Deployment)

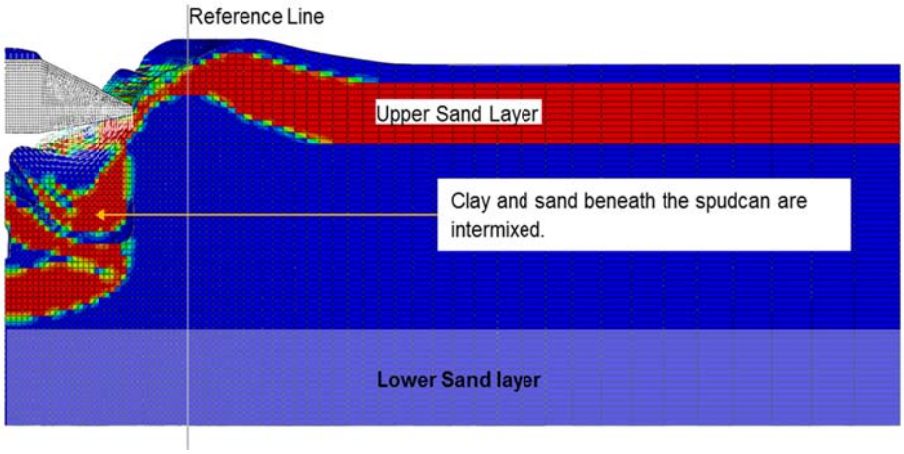

Figure 4a: Spudcan Penetration Depth = 4.5m (Second Jack-up Deployment)

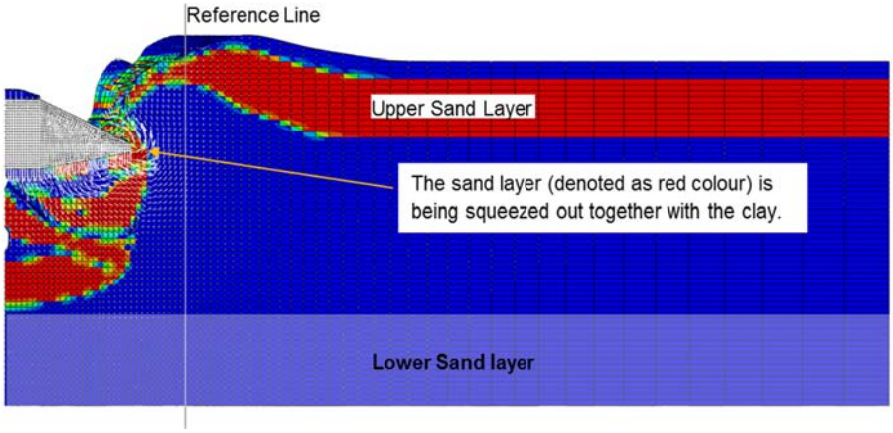

Figure 4b: Spudcan Penetration Depth = 7.5m (Second Jack-up Deployment)

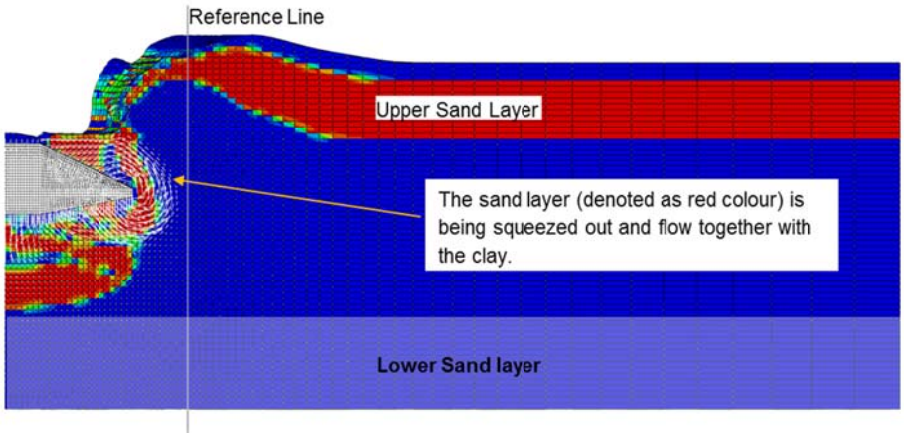

Figure 4c: Spudcan Penetration Depth = 10.5m (Second Jack-up Deployment)

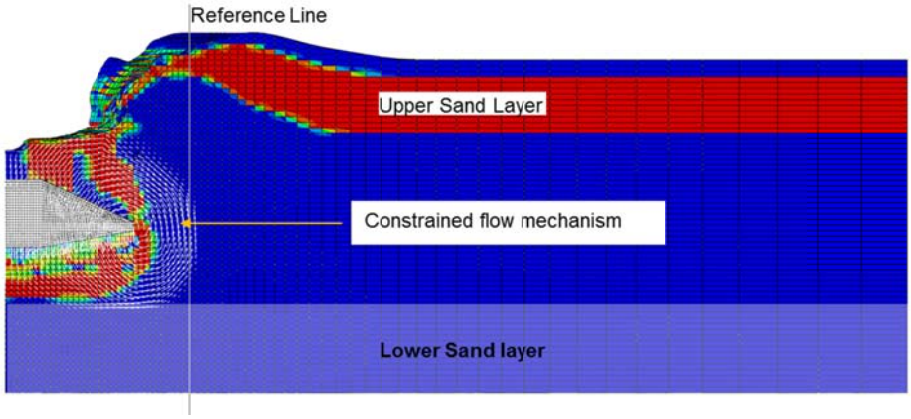

Figure 4d: Spudcan Penetration Depth = 13.5m (Second Jack-up Deployment)

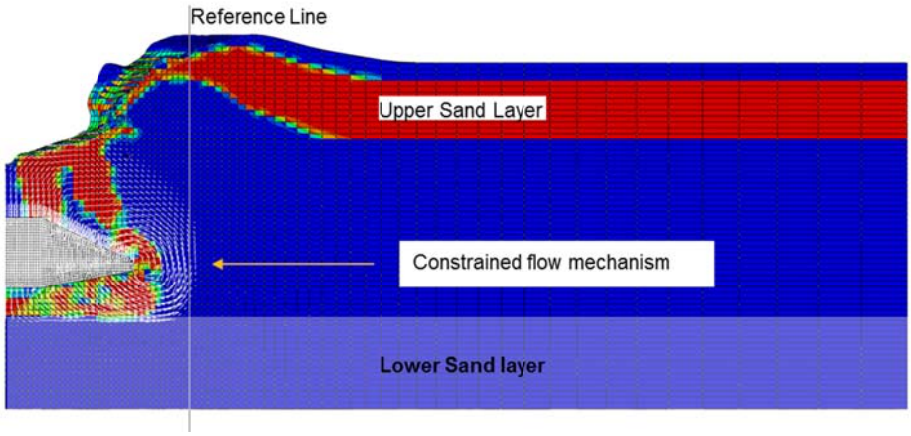

Figure 4e: Spudcan Penetration Depth = 15.6m (Second Jack-up Deployment)

The numerically simulated load-penetration curves and discrete points from field measures during both the first and second jack-up rig deployments are presented in Figure 5. The load-penetration curve corresponding to the virgin soil condition computed using conventional approach (SNAME, 2008) is also presented for comparison.

For the first jack-up rig deployment, the load-penetration curve computed using conventional approach based on SNAME (2008) indicates rapid leg penetration will occur over depths of ~2m to ~17m at close to 100MN spudcan reaction. On the other hand, the LDFE model indicated that leg run will occur from ~4m to ~13m. The actual spudcan penetration measured on site is approximately 13.5m at 100MN spudcan reaction. The LDFE result is found to agree well with the field measured spudcan penetration. On the other hand, the final penetration depth computed based on conventional approach in accordance with SNAME (2008) is about 4m deeper. This can be attributed to the fact that methods detailed in SNAME (2008) and ISO-19905-1(2012) are based on "wished-in-place" simplification which neglects the changes in soil stratigraphy during spudcan penetration. In this case, the sand plug that is extruded as the spudcan penetrates through the upper sand layer and carried down with the spudcan as a composite footing is modelled in the LDFE simulation but neglected in the calculation based on SNAME (2008) approach. The presence of this sand plug beneath an advancing spudcan has the effect of lowering the depth of the equivalent footing and increasing the operative bearing capacity factor and hence resulting in a shallower final penetration.

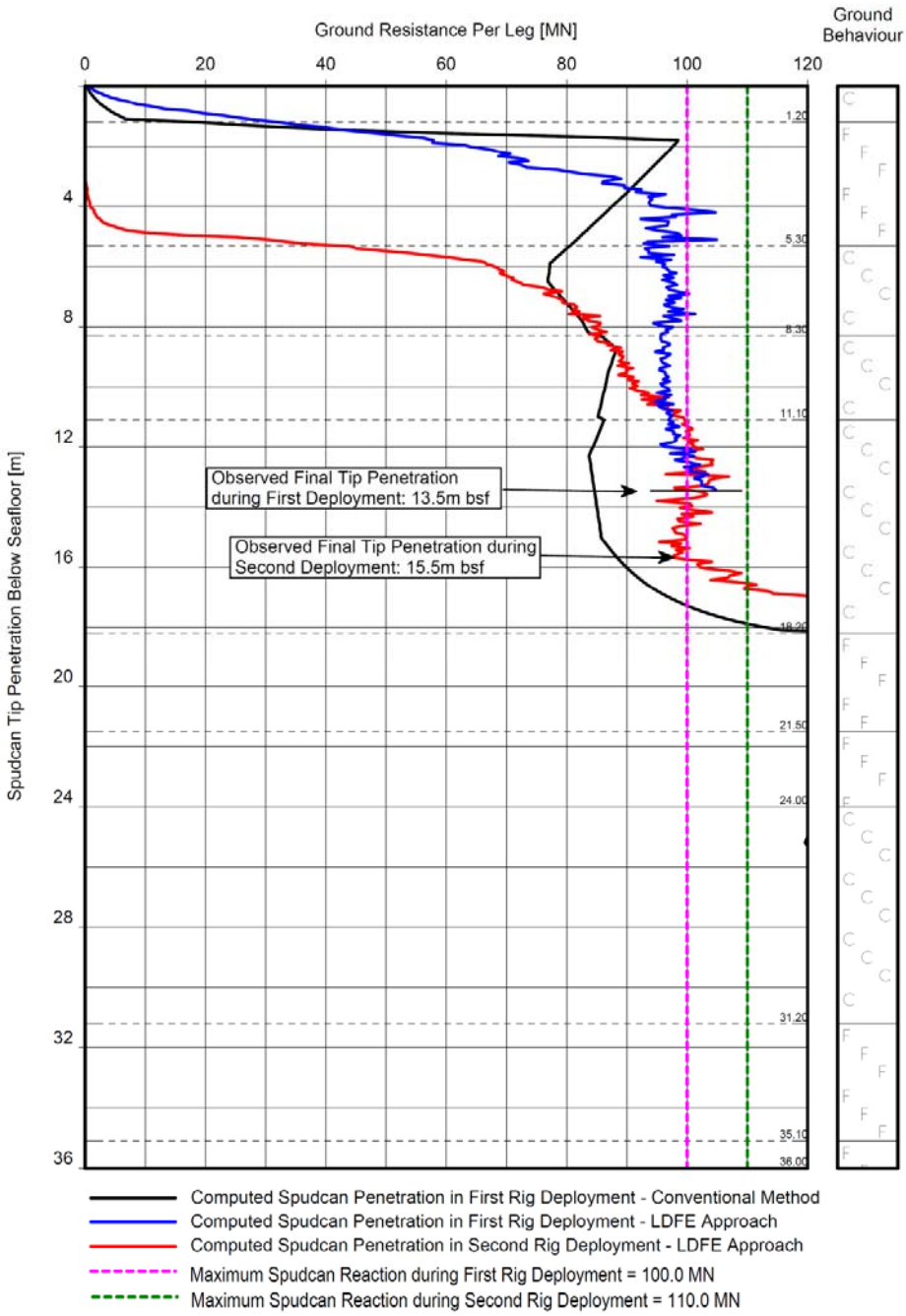

Figure 5: Leg Penetration Curve

For the second jack-up rig deployment, the numerical model correctly predicted that the ground resistance for the top 4.5m is negligible due to the presence of a crater formed after spudcan extraction during the first jack-up rig deployment. The numerically predicted spudcan tip penetration depth at a maximum preload of 110MN during the second jack-up rig deployment is about 17m. This is slightly deeper than the penetration depth of 15.5m observed on site. In the field, the sand layer which collapses into the footprint/crater is likely to loosen up and intermix with sea water and clay. This mixing phenomenon (sand, clay and water), can only be approximately simulated in the numerical model by degrading the operative friction angle of sand that flows into the crater/footprint and hence some discrepancy is expected. It is also interesting to note that despite the

consideration of the effect of soil remoulding in the LDFE model, the LDFE predicted final penetration depth during re-penetration is less that those predicted based on conventional approach using intact soil parameters. This apparent contradiction can be attributed to the relative contribution between the effect of sand plug beneath the spudcan and the effect of strain softening in the clay layers. Overall, the LDFE model is found to be able to replicate the site observations relatively well for both jack-up rig deployments by simulating the changes in soil stratigraphy and strength properties during the first spudcan penetration and extraction process followed by re-penetration during the second jack-up rig deployment.

CONCLUSIONS

This case study demonstrated that the ABAQUS CEL approach is a viable tool for preforming spudcan penetration and re-penetration analysis in layered soil profiles. For computing the spudcan load-penetration response in virgin ground in layered soil profile such as those encountered at this site, the LDFE approach has the advantage of being able to account for the formation and evolution of the sand plug beneath the spudcan. More importantly, the LDFE model is shown to be capable of numerically simulating the formation of a footprint and the associated changes in soil stratigraphy and strength profile by simulating the spudcan extraction process after the first spudcan penetration. When validated against field data, the spudcan re-penetration response is found to be well predicted by the LDFE model.

REFERENCES

[1] Einav I, Randolph MF, Combining upper bound and strain path methods for evaluating penetration resistance, International Journal for Numerical Methods in Engineering. 2005:63(14):1991-2016.

[2] Lee KK, Investigation of Potential Spudcan Punch-Through Failure on Sand Overlying Clay Soils, PhD thesis, University of Western Australia. 2009.

[3] Qiu G, S Henke, J Grabe, Application of a Coupled Eulerian-Lagrangian approach on geomechanical problems involving large deformations, Computers and Geotechnics. 2011:38(1):30-39.

[4] SNAME, Guidelines for site specific assessment of mobile jackup units, Society of Naval Architects and Marine Engineers, Technical and Research Bulletin 5-5A. New Jersey, 2008.

[5] Teh KL, Cassidy M, Leung CF, Chow YK, Randolph MF, Quah C, Revealing the bearing capacity mechanisms of a penetrating spudcan through sand overlying clay, Geotechnique. 2008:58(10):793-804.

[6] Tho KK, Leung CF, Chow YK, Swaddiwudhipong S, Eulerian Finite-Element Technique for Analysis of Jack-Up Spudcan Penetration, International Journal of Geomechanics. 2012:12(1):64-73.

[7] Wang D, White DJ, Randolph MF, Numerical simulations of dynamic embedment during pipe laying on soft clay. In: 28th International Conference on Ocean, Offshore and Arctic Engineering (OMAE2009). USA: New York, CD, 2009.p OMAE2009-79199.

[8] Zhou H, Randolph MF, Computational techniques and shear band development for cylindrical and spherical penetrometers in strain-softening clay, International Journal for Geomechanics. 2007:7(4):287-295.